2008

From shell to cell: neutron scattering studies of biological water dynamics and coupling to activity

A. Frölich
Institut de Biologie Structurale, France

F. Gabel
Institut de Biologie Structurale, France

M. Jasnin
Institut Laue Langevin, France

U. Lehnert
Institut de Biologie Structurale, France

D. Oesterhelt
Max Planck Institut für Biochemie, Germany

See next page for additional authors

From shell to cell: neutron scattering studies of biological water dynamics and coupling to activity

Abstract

An integrated picture of hydration shell dynamics and of its coupling to functional macromolecular motions is proposed from studies on a soluble protein, on a membrane protein in its natural lipid environment, and on the intracellular environment in bacteria and red blood cells. Water dynamics in multimolar salt solutions was also examined, in the context of the very slow water component previously discovered in the cytoplasm of extreme halophilic archaea. The data were obtained from neutron scattering by using deuterium labelling to focus on the dynamics of different parts of the complex systems examined.

Keywords

Water dynamics, Neutron scattering

Publication Details

This article originally published as Frolich, A, Gabel, F, Jasnin, M, Lehnert, U, Oesterhelt, D, Stadler, A, Tehei, M, Weik, M, Wood, K and Zaccai, G, From shell to cell: neutron scattering studies of biological water dynamics and coupling to activity, Faraday Discussions, 141, 2008, 117-130. Copyright Royal Society of Chemistry 2008. Original article available here

Authors

A. Frölich, F. Gabel, M. Jasnin, U. Lehnert, D. Oesterhelt, A. Stadler, M. Tehei, M. Weik, K. Wood, and G. Zaccai

Address for correspondence:

G. Zaccai, Institut Laue Langevin, 6 rue Jules Horowitz - BP 156, Grenoble Cedex 9, France. Telephone: +33476207679, e-mail: zaccai@ill.fr.

From shell to cell: neutron scattering studies of biological water dynamics and coupling to activity†

A. Frölich[1, ‡], F. Gabel[1], M. Jasnin[2], U. Lehnert[1, §], D. Oesterhelt[3], A. Stadler[2], M. Tehei[2, #], M. Weik[2], K. Wood[1, 2, ¶], G. Zaccai[2, *]

†) All the authors contributed equally to the work

*) Presenting author, zaccai@ill.fr

1) Institut de Biologie Structurale, Grenoble, France

2) Institut Laue Langevin, Grenoble, France

3) Max Planck Institut für Biochemie, Martinsried, Germany

§) Present address: McKinsey & Co., London, UK

¶) Present address: University of Groningen, The Netherlands

‡) Present address: Universität Karlsruhe, Germany

#) Present address: University of Wollongong, Australia

Abstract

An integrated picture of hydration shell dynamics and of its coupling to functional macromolecular motions is proposed from studies on a soluble protein, on a membrane protein in its natural lipid environment, and on the intracellular environment in bacteria and red blood cells. Water dynamics in multimolar salt solutions was also examined, in the context of the very slow water component previously discovered in the cytoplasm of extreme halophilic archaea. The data were obtained from neutron scattering by using deuterium labelling to focus on the dynamics of different parts of the complex systems examined.

Key words: hydration, bacteriorhodopsin, purple membrane, deuterium labelling, lipid-membrane protein interaction, maltose binding protein, NaCl and KCl solutions, *E. coli*, red blood cells, *H. marismortui*

Abbreviations: BR, bacteriorhodopsin; PM, purple membrane; MBP, maltose binding protein; RBC, red blood cell; PM H-BR/H-lip, H-BR/D-lip and D-BR/H-lip, reconstituted PM, respectively hydrogenated BR/hydrogenated lipid, hydrogenated BR/deuterated lipid, deuterated BR/hydrogenated lipid.

Introduction

Understanding the dynamic state of water in biological systems and its influence on macromolecular activity is a major scientific challenge. The huge diversity displayed by living organisms is based on a few unifying principles. All known living organisms are constituted of cells or have been through a cellular stage. They require the full set of a variety of macromolecules of specific chemical type (DNA, RNA, proteins…), ions, specific small molecules, and water, in order to thrive and reproduce. Life on Earth has colonized every possible niche in conditions that span extremes in solvent salinity and pH values, temperature and pressure. A scoop of soil, a sample of water, of ice, of air or even of rock from just about anywhere on Earth—including the poles, the tops of the highest mountain ranges, the deepest ocean trenches, neutral or alkaline salt lakes, or very hot acidic volcanic springs—are all likely to reveal biological activity. Ice usually has liquid inclusions, and organisms that live at temperatures well above 100ºC are under high pressure, in which the water is still liquid. As was debated at a Royal Society discussion published in 2004[1], the availability of liquid water may well be the only environmental requirement for Life. The extreme halophilic archaea live in salt lakes and saline ponds in essentially saturated salt water; they counterbalance the osmotic pressure due to the external multimolar NaCl concentration by accumulating multimolar KCl in their cytoplasm. Considering the inside of a cell is already very crowded with macromolecules, which occupy close to 30% of its volume, what is the state of the water compared to that in the bulk liquid? There are about 55 moles in a

kilogramme of water. In a six molal solution of a fully ionised monovalent salt, therefore, there are 4.5 water molecules per ion. Ions may be coordinated by six water molecules, so that each and every water molecule has at least one ion as one of its nearest neighbours, leading to significantly reduced water activity. The existence of extreme halophiles proves that Life has adapted to reduced water activity, but there is no evidence that water can be done away with altogether in biological activity.

In this paper, we present and discuss results on water dynamics in different biological systems, and on the coupling between biological activity and the environment around macromolecules: water in the case of soluble proteins, water and lipids in the case of membrane proteins.

Neutron scattering is a particularly suited experimental technique to probe water dynamics under different conditions. Slow neutrons scatter off bound protons exchanging energy in the thermal range corresponding to the picosecond-nanosecond (ps-ns) time-scale, and momentum corresponding to the 0.1 nm length-scale. Energy resolved incoherent neutron scattering, especially in the elastic (EINS) and quasielastic (QENS) scattering modes, have been informing us on water dynamics under different conditions for decades. Because the method relies on incoherent scattering, samples need not be crystalline or even monodisperse and measurements can be performed on highly complex systems such as living cells[2] or stacks of natural

membranes[3]. The incoherent neutron scattering cross section of hydrogen is more than an order of magnitude larger than that of other atomic nuclei usually found in biological material and their isotopes, including deuterium, and the development of *in vivo* specific deuterium labelling methods permitted the focus on water dynamics in complex biological samples, and its coupling with biological function and activity.

While a consensus has emerged that water molecules close to protein surfaces are dynamically slowed down with respect to bulk water molecules, quantitative aspects and the mechanisms involved remain the objectives of active research (reviewed by Ball[4]). Reports on the dynamics of water molecules close to protein surfaces measured by neutron spectroscopy were presented at a previous Faraday Discussion[5, 6]. The factors found for the slowing down of the diffusion coefficient of hydration water compared to bulk water varied between 2 and 100, depending on the protein, temperature and hydration conditions. Bon et al.[7] studied hydration water in lysozyme crystals by QENS. They distinguished two water populations, denoted as "first" and "second" hydration shells, with diffusion coefficients slowed down by a factor of 10 and 50 compared to bulk water, respectively. By combining EINS data from two spectrometers, Gabel and Bellissent-Funel[8] reported diffusion coefficients of deuterated C-Phycocyanin hydration water, in the presence of trehalose molecules, which are slowed down by a factor of 10-15 with respect to bulk water. As has been pointed out, however, in Gabel et al.[9] and by Gabel and Bellissent-Funel[8], results

obtained at different energy resolutions, different wave vector transfers and using different fit models are not directly comparable.

On the scale of the biological cell, water constitutes the malleable matrix that envelops and sustains intracellular components and biological activity. Considering that macromolecular concentration in the cytoplasm can reach 400 mg/ml, to what extent is water dynamics perturbed by steric confinement between macromolecular surfaces? Does the cell 'tame' water behaviour as some believe (reviewed by Ball[4])? While widely differing opinions concerning the dynamic state of water in the cell are represented in the biology community, there has been very little work on atomic scale measurements of intracellular water dynamics in close to physiological conditions. Below, we present and discuss recent neutron scattering experiments performed on different cell systems, which shed light on *in vivo* intracellular water dynamics.

Hydration water is an integral and essential part of a protein structure. Without it the macromolecule would not be folded correctly. It is essential for the protein to fulfil its biological function. Devoid of hydration water, proteins are inactive[10] and lack essential motions, thus implicitly suggesting a close relationship between protein and hydration water dynamics. The term 'slaving' has been used to express that water can impose its dynamical fingerprint on a protein[11, 12]. Cryo-temperature dependent neutron scattering experiments revealed the solvent dependence of dynamical

transitions in soluble proteins[13-21] and in RNA[22] and provided insights into the coupling between them. Molecular dynamics simulations suggested the onset of water translational diffusion to be at the origin of the dynamical transition[23, 24]. In contrast, however, the onset of hydration water translational diffusion at 200 K, in a membrane, was not observed to trigger a dynamical transition in the membrane protein[25, 26], suggesting a more complex interaction between protein, water, and the membrane lipid environment. Recent neutron scattering studies, using specific deuterium labelling, confirmed that a dynamical transition coincides with the onset of hydration water translational diffusion, in the case of a soluble proteins[27], but not in the case of a membrane protein[3, 28].

By using specific deuteration and samples with controlled hydration, water dynamics was measured directly by neutron scattering in the hydration shell around a soluble protein, and a natural membrane and correlated with macromolecular dynamics, as well as *in situ* in prokaryotic and red blood cells.

Maltose binding protein (MBP) is a soluble monomeric protein of 41 kDa. It plays an essential role in the metabolism of *E. coli*[29]. *In vivo* deuteration of MBP allowed the direct extraction of hydration water dynamics in neutron scattering experiments on the deuterated protein hydrated in H_2O. Water dynamics thus obtained were compared to protein dynamics obtained by measuring natural abundance MBP in D_2O[27].

The purple membrane (PM) of *H. salinarum* is formed of a highly ordered two-dimensional lattice of archaeal specific lipids and the retinal binding protein, bacteriorhodopsin (BR)[30]. BR functions as a light-driven proton pump. Its activity can be followed quite sensitively by spectroscopic methods because it is associated with a millisecond photocycle of protein conformational changes and retinal colour changes. Integral membrane proteins are active in a complex environment constituted of lipid hydrocarbon chains, lipid head groups and hydration water in contact with different parts of the protein. By using fully deuterated membranes hydrated in H_2O and natural abundance membranes hydrated in D_2O, the coupling between hydration water and membrane dynamics has been explored[3, 28]. In another set of experiments, the dynamic coupling between membrane protein and lipids was observed by applying *in vivo* deuterium labelling and *in vitro* reconstitution of PM. The samples allowed the observation of the lipid and protein dynamics, separately.

In vivo neutron scattering measurements in the cytoplasm of deuterated prokaryotic organisms revealed very different water dynamics behaviour in bacteria and extreme halophilic archaea. In order to examine the effect of the high salt environment within halophilic archaea, water dynamics was measured in saturated KCl and NaCl solutions. Water dynamics inside red blood cells (RBC), which contain mainly the equivalent of a 300 mg/ml solution of hemoglobin, was also measured.

The joint analysis of the results allowed us to propose a coherent view of water

dynamics in the hydration shell, the lipid environment of a membrane protein, and the intracellular milieu in various cell types, as well as of the dynamic coupling between biological activity and environment.

Materials and Methods

Samples. The expression and purification of deuterated and natural abundance MBP has been described before[27]. For neutron scattering experiments, powders of deuterated and natural abundance MBP were hydrated to a level of 0.4 g water / g MBP in H_2O and D_2O, respectively (for details see Wood et al.[27]).

PM was extracted from natural abundance or fully deuterated cultures of *H. salinarum* as described before[31, 32]. The experiments were performed on membrane-water stacks in H_2O or D_2O with lamellar spacings of 54 Å, corresponding to an inter-membrane water layer of 5 Å, and a hydration level of approximately 0.1 g water / g membrane[28]. The specifically labelled lipid and BR samples were prepared by delipidation and reconstitution as described in detail by Lehnert[33]. Three reconstitutions were prepared: (i) a control sample of hydrogenated BR and hydrogenated lipids (H-BR/H-lip or H/H); (ii) a sample with hydrogenated BR and deuterated lipids (H-BR/D-lip or H/D); (iii) a sample with deuterated BR and hydrogenated lipids (D-BR/H-lip or D/H). Several parameters were tested in order to find optimum reconstitution conditions. When the buoyant density (from a sucrose gradient) of the fully hydrogenated reconstitution (H/H) corresponded to native PM, the conditions were considered as correct and applied to the hybrid deuterated PM samples. The experimental values agreed well with the expected ones indicating that the lipid/BR ratio corresponded to that in natural PM. X-ray and neutron diffraction indicated poor lattice formation in the reconstituted samples. Light induced cross-linking indicated that the probability of trimer formation in the reconstituted sample

was smaller compared to dimer formation, in contrast to native PM. The UV absorption spectrum indicated a shift of the bound retinal peak to 567 nm, compared to 570 nm in native PM, as observed before in reconstituted samples. The lipid composition of the reconstituted samples was investigated in the negative-ion mode of electrospray ionisation (ESI) mass spectrometry. Traces of hydrogenated phospho- and glyco-lipids were observed indicating that they were not removed during the delipidation process. The hydrogenated contribution accounted for about 5% of the total. It arises from lipid strongly associated to the protein and that was not removed in the delipidation process. The special interaction between the glycolipids and the protein has been discussed by Weik et al.[34].

Deuterated *E. coli* (BLE21(DE3) strain) were cultivated as described previously[35]. Cell pellets containing H_2O or D_2O buffer were prepared in such a way as to reduce strongly the quantity of extracellular water in the sample, which was found to represent less than 7 % of the total water (see Jasnin et al.[35] for details).

Deuterated *H. marismortui* cells were grown at 37°C to an optical density of 0.8–1 (late logarithmic phase) in medium described before[36], in which yeast extract was replaced by deuterated algal extract produced at the Max Planck Institut für Biochemie (Martinsried, Germany). For neutron scattering experiments, cells were pelleted in D_2O or H_2O buffer (see Tehei et al.[36] for details).

For the RBC experiments, samples of human venous blood were taken from healthy adults. The cells were washed with phosphate buffer solution (PBS) and were gassed with CO to increase the stability of hemoglobin. The glycocalyx matrix was removed as described elsewhere[37]. Half of the cells were then washed with D_2O PBS buffer until the level of H_2O was below 0.1%. No cell lysis was detected during the preparation and the shape of the cells was checked with optical microscopy.

Neutron scattering. Elastic incoherent neutron scattering (EINS) experiments provide information on atomic mean square displacements (MSD) in a sample as a function of temperature[38]. The time-scale examined (0.1 ns on IN13 (http://www.ill.eu/in13/home/), and 1 ns on IN16 (http://www.ill.eu/in16/home/) at the Institut Laue Langevin (ILL) depends on the energy resolution of the spectrometer, while the scattering vector, Q, range, in which the scattered intensity is measured, defines the length-scale (down to less than 1 Å for IN13 and of the order of 1 Å for IN16). Plots of MSD as a function of absolute temperature are called elastic scans. MSD are in absolute $Å^2$ units. An effective dynamic resilience expressed as an elastic force constant (in Newtons per metre) can be calculated from the inverse of the slope of $< u^2 >$ versus T[38, 39]. Elastic scans for proteins and membranes usually show a break in slope at about 200 K, which has been interpreted as a dynamical transition from a harmonic low temperature regime to an anharmonic regime that has been modelled, for example, by a double-well free energy potential[15]. In a quasi-harmonic approximation, the dynamical transition is associated with a

significant decrease in resilience.

An exhaustive description of quasielastic incoherent neutron scattering (QENS) can be found in Bée[40]. QENS is measured as a function of both energy transfer and scattering vector, Q. On the energy scale, the elastic scattering appears as a peak centered on zero energy transfer whose width corresponds to the spectrometer resolution. The QENS appears as a significantly broader peak, also centered on zero energy transfer. The shape of the QENS peak and its Q variation contain information on the time and geometry associated with the motion of the scattering particle. In the case of simple exponential diffusion processes, the QENS spectra can be fitted mathematically by Lorentzian functions. By applying various models such as the jump diffusion, Singwi-Sjölander and Sears models (see Bée[40] for details), to fit the Lorentzian width as a function of Q, it is possible to calculate rotational relaxation and correlation times, translational residence time, and translational and rotational diffusion coefficients for the scattering particle.

Results

Hydration water dynamics and coupling to the soluble maltose binding protein from *E. coli.* Water structure[41, 42] and dynamics[5, 8, 9] at the vicinity of a soluble protein surface are different than in the bulk liquid state. MBP powders hydrated at 0.4 g water / g protein contain one hydration layer per protein molecule. The deuterated MBP in H_2O gave access to the dynamics of hydration water, which contributes 73% to the total incoherent scattering cross section but only 2% in natural abundance MBP in D_2O. The MSD of water and protein motions, plotted in Figure 1A, are similar up to 220 K, at which temperature they both exhibit a transition[27]. Above 220 K, the water MSD are above those of the protein.

Hydration water dynamics in purple membrane and coupling to bacteriorhodopsin and membrane lipids. PM stacks were hydrated to a level that corresponds to one hydration layer per membrane surface (i.e. 5 Å of inter-membrane water). EINS experiments on deuterated PM hydrated in H_2O permitted to access the dynamics of the first hydration layer directly. In the sample, 60% of the total incoherent scattering cross section was calculated to be due to the contribution of inter-membrane water. In contrast, as with the MBP samples discussed above, in natural abundance PM hydrated in D_2O the contribution from hydration water is negligible and the total incoherent scattering cross section is strongly dominated by the PM (77% BR protein, 23% lipids), thus reflecting membrane dynamics. The elastic temperature scans are presented in Figure 1B[28]. Hydration water MSD

increase linearly up to 200 K, at which temperature there is a break in slope suggesting a dynamical transition in water dynamics. The PM MSD show breaks in slope at 120 and 260 K, but not at 200 K.

The *in vitro* reconstituted PM samples were characterised by UV spectrophotometry, cross-linking experiments for BR trimer formation, mass spectrometry for lipid composition and deuterium labelling, and X-ray diffraction for lattice formation and order (see *Materials and Methods*). Studying the reconstituted hydrogenated BR and hydrogenated lipids sample (H-BR/H-lip) probed the global dynamics of the whole membrane (68% of the incoherent scattering cross section is from BR, 31% from lipids), whilst in the hydrogenated BR, deuterated lipid sample (H-BR/D-lip) BR clearly dominated the signal (98%). Using deuterated BR with hydrogenated lipids (D-BR/H-lip) provided information on the lipid dynamics, which represent 92% of the incoherent scattering cross section. Figure 2 presents the atomic mean square displacements (MSD) measured for the H-BR/H-lip and D-BR/H-lip reconstituted samples at 93% relative humidity, which represent, respectively, dynamics of global PM and of the native archaeal lipids in the membrane on the ns time-scale. The H-BR/D-lip sample MSD are not shown; they were very close and slightly below the H-BR/H-lip values, as expected from the BR:lipid ratio in the membrane composition. The MSD of the H-BR/H-lip sample are very similar to those of natural PM. The two dimensional lattice in the reconstituted samples, however, was not as well ordered as in the natural membrane, indicating that membrane internal dynamics in the ns time-

scale is not influenced by lattice order. As seen in Figure 2, between 20 and about 200 K, the MSD of both samples are the same, with a deviation from harmonic behaviour at about 150 K: PM and its lipid components have similar vibrational dynamics at very low temperatures and display the anharmonicity associated with methyl rotations from about 150 K[14, 43]. We recall that PM lipids do not have fatty acid chains but phytol chains that are rich in methyl groups. Above 200 K, the MSD of the two samples become clearly different, with the archaeal phytol chains displaying greatly increased dynamics compared to the average membrane. In both samples shown in Figure 2, further onsets of large amplitude motions occur at 260 K, suggesting coupled increases in dynamics in the lipid and protein components of PM.

Intracellular water dynamics in *E. coli* and red blood cells. *E. coli* water dynamics was studied in fully deuterated cell pellets resuspended in H_2O and D_2O buffers, respectively. A subtraction of the cell spectra measured in D_2O, from the cell spectra measured in H_2O, scaled by the sample mass, provided a good approximation to the scattering signal from the water present in the samples. A sample of H_2O buffer alone was measured as well, and used as a reference for interpreting the data. The measurements were carried out on two neutron spectrometers, IN6 at ILL (energy resolution of 90 μeV, see http://www.ill.eu/in6/home/) and IRIS (energy resolution of 17 μeV, see http://www.isis.rl.ac.uk/molecularSpectroscopy/iris/), to cover diffusive motions from those of bulk to interfacial water. IRIS and IN6 QENS spectra were well fitted using a single and two Lorentzian functions, respectively

(see Jasnin et al.[35] for details). The Lorentzian extracted on IRIS was attributed to translational motions of cell water. Its half-width at half-maximum (HWHM), Γ_T, was extracted and best fitted using a jump diffusion model[40], which describes diffusion between sites for the water protons with a mean residence time, τ_0, at each site. We found the following values for the translational diffusion coefficients, D_T, and associated τ_0: D_T = 1.53 x 10^{-5} $cm^2.s^{-1}$, τ_0 = 2.63 ps at 281 K and D_T = 2.39 x 10^{-5} $cm^2.s^{-1}$, τ_0 = 2.16 ps at 301 K. D_T values are very close to those of bulk water at corresponding temperatures, with residence times about twice longer. The rotational water contribution emerged from the broad Lorentzian extracted from IN6 QENS spectra. We found the following rotational correlation times, $\tau_{cor,R}$: $\tau_{cor,R}$ = 1.96 ps at 281 K, and 1.54 ps at 301 K. The values were close to the values extracted for the buffer under the same conditions and of the same order as the values measured for bulk water by QENS[44] and NMR[45]. From the two sets of data, we concluded that *E. coli* water dynamics is dominated by a bulk-like water component at physiological temperature. A similar conclusion was reached for water in RBC, indicating that the result was not restricted to bacteria (see below).

The diffusion of cytoplasmic water in whole human RBC was measured by QENS. RBC grow in the bone marrow of mammals, and deuterated material is not available so far. Natural abundance cells were measured in H_2O and D_2O buffers with high precision and the scattering data were subtracted from each other, to yield intensities representing the dynamics of water only. As a reference, H_2O buffer solution was

measured. The experiment was performed on the time-of-flight neutron spectrometer TOFTOF[46] at the Munich FRM2 reactor, with an energy resolution of 100 μeV, in the temperature range 290 K to 320 K. The measured spectra in the *Q*-range from 0.5 $Å^{-1}$ to 1.5 $Å^{-1}$ were well fitted from -1.5 meV to +1.5 meV with a narrow and a broad Lorentzian function plus linear background, corresponding to translational and rotational motions of the water molecules, respectively. The HWHM profile as a function of Q^2 of the narrow Lorentzian are in agreement with a jump diffusion model[40]. The translational diffusion coefficient, D_T, and the residence time, τ_0, of water were obtained from the fits. The diffusion coefficients of cytoplasmic water are only slightly reduced compared to those obtained for the buffer solution, but interestingly the residence times of cytoplasmic water are in average five times higher than in buffer solution (details are given in Stadler et al.[47]).

Extreme halophiles: a special case? Intracellular water dynamics in *H. marismortui*, an extreme halophile originally isolated from the Dead Sea, was studied by QENS. Water motions in centrifuged cell pellets were measured by means of two spectrometers, IN6 (http://www.ill.eu/in6/home/) and IN16 (http://www.ill.eu/in16/home/), sensitive to motions with time-scales of 10 ps and 1 ns, respectively. From IN6 time-of-flight (energy resolution of 100 μeV) data, using the model of Singwi and Sjölander[48], a translational diffusion constant of 1.3 x 10^{-5} $cm^2.s^{-1}$ was determined at 285 K for *H. marismortui* cells. The value is close to that found previously for other cells and close to that for bulk water, as well as that of the

water in the 3.5 M NaCl solution bathing the cells[49]. A very slow water component was discovered from the IN16 data (energy resolution of 0.9 μeV). At 285 K, the values of HWHM are independent on Q^2. The water protons of this component displayed a residence time of 411 ps (compared with a few ps in bulk water). At 300 K, the residence time dropped to 243 ps and was associated with a translational diffusion of 9.3 x 10^{-8} $cm^2.s^{-1}$, or 250 times lower than that of bulk water. The slow water accounts for about 76% of cell water in *H. marismortui*. No such slow water was found in *E. coli*, measured on the BSS backscattering spectrometer (energy resolution of 0.9 μeV, at the Jülich Neutron Centre (see http://www.jcns.info/)). It was hypothesized that the slow mobility of a large part of *H. marismortui* cell water indicates a specific water structure responsible for the large amount of K^+ bound within these extreme halophilic cells.

In order to estimate the influence of the solvent ions on the intracellular water dynamics in the extreme halophiles, we studied the diffusion coefficients of water in molar solutions of KCl and NaCl by QENS. To this end, a 3M KCl and a 4M NaCl (each at 50 mM Tris, pH = 7.6, T = 298 K) were measured on the instrument IN5 at the ILL (http://www.ill.eu/in5/), at an energy resolution of 63 μeV (λ = 6 Å) in the wave vector range 0.26 < Q [$Å^{-1}$] < 1.87. The quasielastic spectra were fitted in the energy transfer range -0.5 to +0.5 meV with a scattering law constituted of a linear background, an elastic intensity and a single quasielastic contribution, interpreted within the Singwi-Sjölander model[48]. The model assumes that individual water

molecules diffuse during a time τ_1 and vibrate during a time τ_0 around an equilibrium position. In the approximation $\tau_1 >> \tau_0$, we extracted the apparent diffusion coefficient, D_{app}, from the HWHM of the QENS spectra as a function of Q (Figure 3).

The following apparent diffusion coefficients (combining translational and rotational motions) were measured (the bulk water value is from the literature): D_{app} (4M NaCl in H_2O, T = 298 K) = 1.5 x 10^{-5} $cm^2.s^{-1}$; D_{app} (3M KCl in H_2O, T = 298 K) = 2.0 x 10^{-5} $cm^2.s^{-1}$ and D_{app} (bulk water[5], T = 298 K) = 2.3 x 10^{-5} $cm^2.s^{-1}$. The results showed clearly that the presence of molar salt concentration of NaCl or KCl affects hardly the diffusive properties of water. The findings supplement QENS data published earlier at different salt concentrations and temperatures[50]. Only a weak dependence of the water diffusion coefficient on NaCl concentration (up to 6 M NaCl) was found. In the case of KCl (up to 3.2 M), the diffusion coefficient was similar to that of bulk water. Furthermore, characteristic water frequencies (in the range from 100 to 1000 cm^{-1}) persisted up to 4.6 M KCl and 0.5 M NaCl, respectively. It is only in the case of very small or highly charged ions (Li^+, Mg^{2+}, La^{3+}, etc) that the authors could find a decrease of the water diffusion coefficient at higher concentrations (> 1 M).

It can be concluded that the presence of high salt concentrations in the cytoplasm of extreme halophilic archaea, multimolar NaCl and KCl, is not responsible by itself for the very slow water component observed by Tehei et al.[36].

Discussion

The hydration shell is vital to a macromolecule's biological activity. Without hydration water, proteins would lack not only their correctly folded structure but also the conformational flexibility that *brings them to life* and allows their biological activity. Consequently, protein and hydration water dynamics are supposed to be intimately coupled. One way of exploring the coupling has exploited the so-called protein dynamical transitions, characteristic changes in MSD that appear in at temperatures between about 180 K and 250 K. Do hydration water MSD show similar behaviour, and if so, does the 'transition' temperature coincide with the protein dynamical transition temperature? The questions were addressed in the soluble MBP[27] and in PM[3, 28], by using neutron scattering combined with deuterium labelling to examine the dynamics of each component separately. The first layer of hydration water in both PM and MBP showed a characteristic change in MSD at temperatures between 200 and 220 K (Figure 1) that was attributed to the onset of translational diffusion[3, 27] as proposed earlier[23]. Water and protein transitions in MBP appeared at the same temperature (Figure 1A), as expected from the intimate coupling between hydration water and soluble protein dynamics, which has been reported frequently in the literature (see e.g. Doster et al.[15]; Cordone et al.[51]; Fitter[16]; Reat et al.[19]; Tsai et al.[21]; Vitkup et al.[52]; Zaccai[38]; Paciaroni et al.[18]; Fenimore et al.[11]; Chen et al.[13]; Roh et al.[20]; Swenson et al.[53]; Joti et al.[17]; Doster[14]). In the case of PM, however, the hydration water and membrane transitions were found to be separated by as much as 60 K (Figure 1B). The onset of water translational motion in

the first[3, 28] and second[25, 26] hydration layers at 200 K did not trigger a dynamical transition in PM. The data from specifically labelled reconstituted PM permitted the separated observation of lipid and BR dynamics and showed that the membrane protein dynamics is coupled to the dynamics of its lipid environment, as has been suggested[54, 55], rather than to that of inter-membrane hydration water. The lipid component of PM constitutes only 25% of the membrane mass, and most of the lipid molecules are in contact with protein. The neutron data nevertheless established that the lipids in PM, above 200 K, display higher MSD and softer resilience than BR (Figure 2). As discussed above, 200 K is the temperature of onset of hydration water translational diffusion. It appears, therefore, that lipid dynamics responds to the water. At 260 K there is another break in the MSD of the lipids towards a domain of even smaller resilience (larger slope with temperature), which coincides with a similar dynamic transition in BR. Early neutron diffraction experiments on PM, using H_2O/D_2O exchange to highlight water location, and their comparison with data from lipid bilayer models, had shown the extent of hydration penetrating into the membrane around lipid head groups, and its dependence on the relative humidity of the sample environment[56], [57]. Following these structural observations and the observation that PM activity was inhibited in the dry membrane, it has been speculated that a flexible lipid environment induced by high head group hydration was essential for BR functional dynamics[54]. The parallel transitions in the lipid and BR MSD data at 260 K, observed in the reconstituted PM samples (Figure 2), supports the hypothesis. At 200 K, the onset of translational diffusion in inter-

membrane hydration water apparently induced some flexibility in the membrane lipids but not sufficiently to free high amplitude protein motions. At 260 K, perhaps related to a 'melting' of head group hydration water, both the lipid and BR components of the membrane display a dynamical transition to lower resilience, high amplitude MSD motions.

At the intracellular level, the studies on *E. coli* and RBC revealed that water dynamics is similar to the dynamics of water in the bulk state (Figure 4D). Our studies contributed to dismantle the concept that the cell somehow 'tames' water by modifying its dynamics compared to bulk water[58]. They confirmed the importance of hydration degree for water dynamics in confined geometries; in deuterated C-phycocyanin, for example, increasing water mobility had already been observed when hydration coverage reached one water layer[59]. The first macromolecular hydration layer accounts for about 0.4 to 0.5 g of water per g of macromolecule. Macromolecular concentrations in *E. coli* and RBC correspond to about 300 to 400 mg/ml, *i.e.* to four to six water layers around macromolecular surfaces. The analysis established that because of the relatively high hydration level and resulting low water confinement, intracellular water forms a network of communication that is as fluid as bulk water. In both *E. coli* and RBC, however, residence times were found to be increased by a factor of 2 and 5, respectively, suggesting that water molecules spend longer times in the first hydration shell of macromolecular structures than in the bulk phase.

The extreme halophilic archaea appeared to present an exceptional case with respect to cytoplasmic water mobility. The presence of multimolar NaCl and KCl salt concentrations in their cytoplasm is clearly not responsible by itself for the very slow water component observed by Tehei et al.[36] (Figure 3). It was hypothesized that the slow mobility of a large part of *H. marismortui* cell water indicated a specific water structure, which would also be responsible for the large amount of K^+ bound within the extreme halophile cells. The absolute requirement of *H. marismortui* for a high salt environment and its ability to bind potassium ions specifically appear to be closely related to the low mobility of water in the cells. Halophilic proteins have been shown to have special hydration and ion-binding properties associated with an excess of negative charge in carboxylic groups on their surface[60]. The interactions may be similar to those of structured water around potassium ions and protein carboxylic groups observed by MacKinnon[61] in the potassium channel protein. It would be of significant interest to measure water mobility in these systems, in order to assess if similar mechanisms are responsible for the slow water component in the extreme halophile.

Acknowledgements

We thank Heloisa Nunes Bordallo, Bruno Demé, Bernhard Frick, Marek Koza, Mark F. Telling and Michaela Zamponi for their help during data collection at the Institut Laue-Langevin, at ISIS and at the Jülich Neutron Centre. This work was supported by the Commissariat à l'Energie Atomique, the Centre National de la Recherche

Scientifique, the Université Joseph Fourier, an Agence Nationale de la Recherche Grant (project number JC05_45685), the European Union under the DLAB contracts HPRI-CT-2001-50035 and RII3-CT-2003-505925, and The Integrated Infrastructure Initiative for Neuron Scattering and Muon Spectroscopy (NMI3).

References

1. *Phil. Trans. R. Soc. Lond. B*, 2004, **359**.
2. M. Tehei, B. Franzetti, D. Madern, M. Ginzburg, B. Z. Ginzburg, M. T. Giudici-Orticoni, M. Bruschi and G. Zaccai, *EMBO Rep*, 2004, **5**, 66-70.
3. K. Wood, M. Plazanet, F. Gabel, B. Kessler, D. Oesterhelt, D. J. Tobias, G. Zaccai and M. Weik, *Proc Natl Acad Sci U S A,* 2007, **104**, 18049-18054.
4. P. Ball, *Chem Rev*, 2008, **108**, 74-108.
5. M. C. Bellissent-Funel, J. M. Zanotti and S. H. Chen, *Faraday Discuss*, 1996, **103**, 281-294.
6. M. Settles and W. Doster, *Faraday Discuss*, 1996, **103**, 269-280.
7. C. Bon, A. J. Dianoux, M. Ferrand and M. S. Lehmann, *Biophys J*, 2002, **83**, 1578-1588.
8. F. Gabel and M. C. Bellissent-Funel, *Biophys J*, 2007, **92**, 4054-4063.
9. F. Gabel, D. Bicout, U. Lehnert, M. Tehei, M. Weik and G. Zaccai, *Q Rev Biophys*, 2002, **35**, 327-367.
10. J. A. Rupley and G. Careri, *Adv Protein Chem*, 1991, **41**, 37-172.
11. P. W. Fenimore, H. Frauenfelder, B. H. McMahon and R. D. Young, *Proc Natl Acad Sci U S A,* 2004, **101**, 14408-14413.
12. I. E. Iben, D. Braunstein, W. Doster, H. Frauenfelder, M. K. Hong, J. B. Johnson, S. Luck, P. Ormos, A. Schulte, P. J. Steinbach, A. H. Xie and R. D. Young, *Phys Rev Lett*, 1989, **62**, 1916-1919.
13. S. H. Chen, L. Liu, E. Fratini, P. Baglioni, A. Faraone and E. Mamontov, *Proc Natl Acad Sci U S A,* 2006, **103**, 9012-9016.
14. W. Doster, *Eur Biophys J*, 2008.
15. W. Doster, S. Cusack and W. Petry, *Nature*, 1989, **337**, 754-756.
16. J. Fitter, *Biophys J*, 1999, **76**, 1034-1042.
17. Y. Joti, H. Nakagawa, M. Kataoka and A. Kitao, *Biophys J*, 2008.
18. A. Paciaroni, S. Cinelli and G. Onori, *Biophys J*, 2002, **83**, 1157-1164.
19. V. Reat, R. Dunn, M. Ferrand, J. L. Finney, R. M. Daniel and J. C. Smith, *Proc Natl Acad Sci U S A,* 2000, **97**, 9961-9966.
20. J. H. Roh, J. E. Curtis, S. Azzam, V. N. Novikov, I. Peral, Z. Chowdhuri, R. B. Gregory and A. P. Sokolov, *Biophys J*, 2006, **91**, 2573-2588.
21. A. M. Tsai, D. A. Neumann and L. N. Bell, *Biophys J*, 2000, **79**, 2728-2732.
22. G. Caliskan, R. M. Briber, D. Thirumalai, V. Garcia-Sakai, S. A. Woodson and A. P. Sokolov, *J Am Chem Soc*, 2006, **128**, 32-33.
23. M. Tarek and D. J. Tobias, *Phys Rev Lett,* 2002, **88**, 138101.
24. A. L. Tournier, J. Xu and J. C. Smith, *Biophys J,* 2003, **85**, 1871-1875.
25. M. Weik, *Eur Phys J E Soft Matter*, 2003, **12**, 153-158.
26. M. Weik, U. Lehnert and G. Zaccai, *Biophys J,* 2005, **89**, 3639-3646.
27. K. Wood, A. Frolich, A. Paciaroni, M. Moulin, M. Hartlein, G. Zaccai, D. J. Tobias and M. Weik, *J Am Chem Soc*, 2008, in press.
28. K. Wood, M. Plazanet, F. Gabel, B. Kessler, D. Oesterhelt, G. Zaccai and M. Weik, *Eur Biophys J*, 2008, in press.

29. W. Boos and H. Shuman, *Microbiol Mol Biol Rev*, 1998, **62**, 204-229.
30. D. Oesterhelt, *Curr Opin Struct Biol*,1998, **8**, 489-500.
31. D. Oesterhelt and W. Stoeckenius, *Methods Enzymol*, 1974, **31**, 667-678.
32. H. Patzelt, A. S. Ulrich, H. Egbringhoff, P. Düx, J. Ashurst, B. Simon, H. Oschkinat and D. Oesterhelt, *J Biomol NMR*, 1997, **10**, 95–106.
33. U. Lehnert, in *Physics*, Université Joseph Fourier, Grenoble, 2002.
34. M. Weik, H. Patzelt, G. Zaccai and D. Oesterhelt, *Mol Cell*, 1998, **1**, 411-419.
35. M. Jasnin, M. Moulin, M. Haertlein, G. Zaccai and M. Tehei, *EMBO Rep*, 2008, in press.
36. M. Tehei, B. Franzetti, K. Wood, F. Gabel, E. Fabiani, M. Jasnin, M. Zamponi, D. Oesterhelt, G. Zaccai, M. Ginzburg and B. Z. Ginzburg, *Proc Natl Acad Sci U S A*, 2007, **104**, 766-771.
37. A. Elgsaeter and D. Branton, *J Cell Biol*, 1974, **63**, 1018-1036.
38. G. Zaccai, *Science,* 2000, **288**, 1604-1607.
39. D. J. Bicout and G. Zaccai, *Biophys J*, 2001, **80**, 1115-1123.
40. M. Bée, ed., *Quasielastic Neutron Scattering: Principles and Applications in Solid State Chemistry, Biology and Materials Science*, Philadelphia, 1988.
41. F. Merzel and J. C. Smith, *Proc Natl Acad Sci U S A*, 2002, **99**, 5378-5383.
42. D. I. Svergun, S. Richard, M. H. Koch, Z. Sayers, S. Kuprin and G. Zaccai, *Proc Natl Acad Sci U S A*, 1998, **95**, 2267-2272.
43. J. H. Roh, V. N. Novikov, R. B. Gregory, J. E. Curtis, Z. Chowdhuri and A. P. Sokolov, *Phys Rev Lett*, 2005, **95**, 038101.
44. J. Teixeira, M. C. Bellissent-Funel, S. H. Chen and A. J. Dianoux, *Phys Rev A*, 1985, **31**, 1913-1917.
45. G. Sposito, *J Chem Phys*, 1981, **74**, 6943–6949.
46. T. Unruh, J. Neuhaus and W. Petry, *Nucl Instrum Methods Phys Res A*, 2007, 580:1414–1422 and erratum 585:1201.
47. A. M. Stadler, J. P. Embs, I. Digel, G. Artmann, G. Zaccai and G. Büldt, 2008, submitted.
48. K. S. Singwi and A. Sjölander, *Phys Rev*, 1960, **119**, 863-871.
49. B. N. Brockhouse, *Suppl Nuovo cimento* 1958, **9**, 45.
50. P. Leung and G. Safford, *J Phys Chem*, 1970, **74**, 3696-3709.
51. L. Cordone, M. Ferrand, E. Vitrano and G. Zaccai, *Biophys J*, 1999, **76**, 1043-1047.
52. D. Vitkup, D. Ringe, G. A. Petsko and M. Karplus, *Nat Struct Biol*, 2000, **7**, 34-38.
53. J. Swenson, H. Jansson and R. Bergman, *Phys Rev Lett*, 2006, **96**, 247802.
54. G. Zaccai, *J Mol Biol*, 1987, **194**, 569-572.
55. M. Kamihira and A. Watts, *Biochemistry*, 2006, **45**, 4304-4313.
56. G. Zaccai and D. J. Gilmore, *J Mol Biol*, 1979, **132**, 181-191.
57. P. K. Rogan and G. Zaccai, *J Mol Biol*, 1981, **145**, 281-284.
58. P. Mentré, *Cell Mol Biol (Noisy-le-grand)*, 2001, **47**, 709-715.
59. M. C. Bellissent-Funel, J. M. Zanotti and S. H. Chen, *Faraday Discuss*, 1996, **103**, 281-294.

60. D. Madern, C. Ebel and G. Zaccai, *Extremophiles*, 2000, **4**, 91-98.
61. R. MacKinnon, *FEBS Lett*, 2003, **555**, 62-65.
62. B. Frick and M. Gonzalez, *Physica B*, 2001, **301**, 8-19.

Figure legends

Figure 1: (A) Mean square displacements (MSD) of maltose binding protein (MBP) and its hydration water[27]. Dynamic transitions in the hydration water and in MBP take place at similar temperatures (~ 220 K). (B) MSD of purple membrane (PM) and its hydration water[28]. Dynamical transitions take place at 200 K in the hydration water and at 120 and 260 K in PM. The elastic scans were carried out on the IN16 spectrometer with an energy resolution of 0.9 μeV (full-width at half-maximum of the elastic peak and a wavelength of 6.275 Å[62]). MSD were extracted from data in the following Q ranges: $0.2 < Q^2$ [Å^{-2}] < 1.8 for hydrogenated MBP in D_2O (Panel A, *grey circles*), $0.2 < Q^2$ [Å^{-2}] < 1.1 for deuterated MBP in H_2O (Panel A, *black diamonds*), $0.2 < Q^2$ [Å^{-2}] < 1.5 for hydrogenated PM in D_2O (Panel B, *grey circles*), $0.2 < Q^2$ [Å^{-2}] < 0.9 for deuterated PM in H_2O (Panel B, *black diamonds*).

Figure 2: Atomic mean square displacements (MSD) extracted from the analysis of the elastically scattered neutron intensity, measured on the IN16 spectrometer at the ILL (energy resolution (full-width at half-maximum) of 0.9 μeV). The MSD, $< u^2 >$, were calculated using the Gaussian approximation: $I_{el,T}(Q,\omega=0) = A\exp\{- < u^2 > Q^2/6\}$, in which $I_{el,T}$ (Q, $\omega = 0$) is the elastically scattered intensity at a certain temperature T; Q and ω are the momentum and energy transfers, respectively, and A is a constant. Data are shown for the H-BR/H-lip (H/H) and D-BR/H-lip (D/H) reconstituted samples (see *Materials and Methods*). Samples were hydrated to 93% relative humidity in D_2O.

Figure 3: Q^2-dependence of the Lorentzian half-widths at half-maximum (HWHM) extracted from the quasielastic spectra of the multimolar NaCl and KCl solutions. 4M NaCl and 3M KCl solutions were investigated both in D_2O (*top*) and H_2O (*bottom*). The continuous lines represent the fits obtained with the Singwi-Sjölander model[48], which were used to extract the apparent diffusion coefficients.

Figure 4: Summary figure, which shows hydration and coupling 'from shell to cell'. The figure illustrates the main points presented and discussed in the paper, drawn in a large schematic cell. (A) Hydration around a soluble protein and coupling with protein dynamics. (B) Hydration around a membrane not coupled to protein dynamics. (C) Dynamic coupling between protein and lipid in the membrane. (D) Channels of free water flowing around the hydrated macromolecules in the cell and the special case of the extreme halophile.

Figure 1

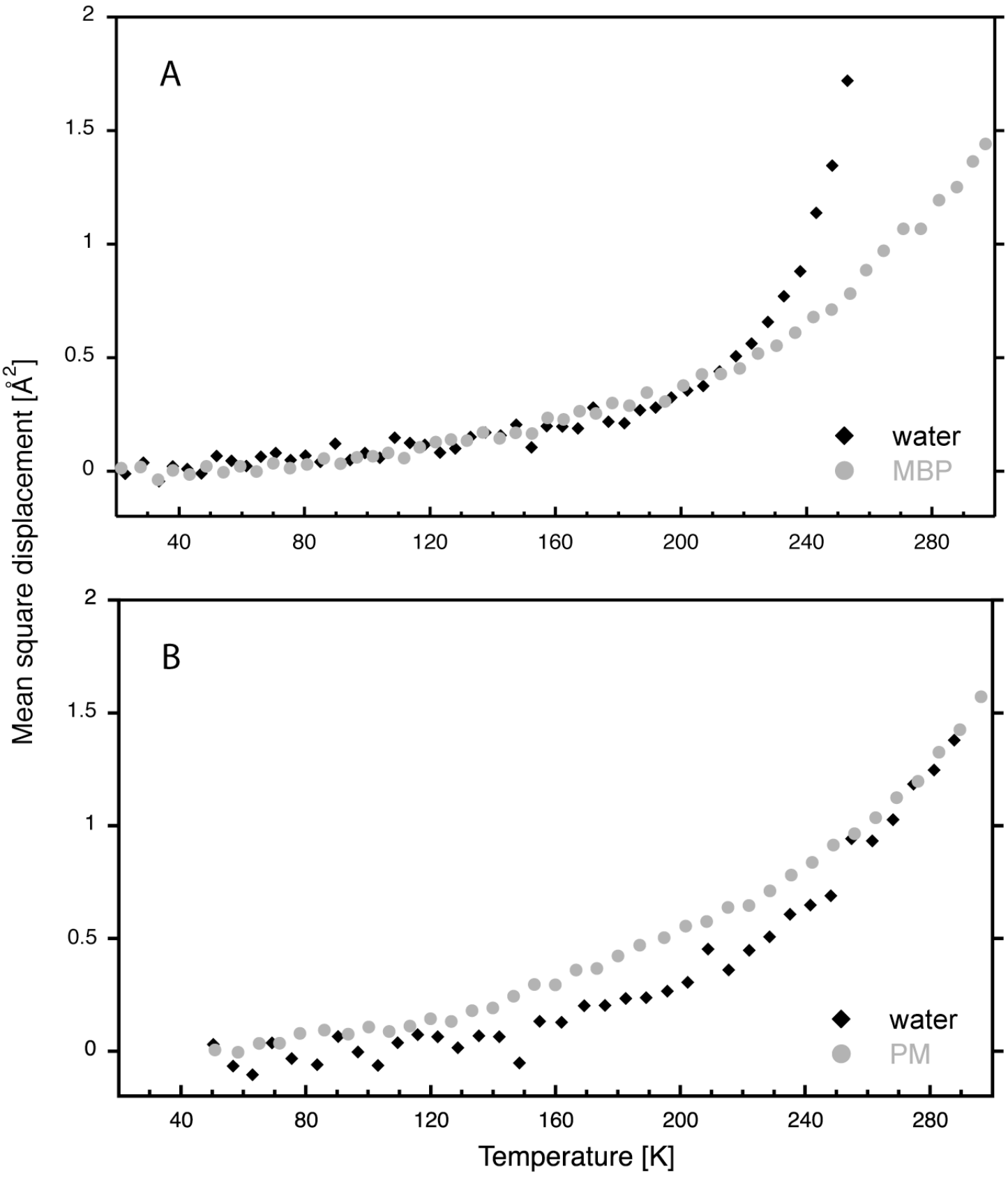
A
B
water
MBP
PM
Mean square displacement [Å^2]
Temperature [K]
0
0.5
1
1.5
2
40
80
120
160
200
240
280

Figure 2

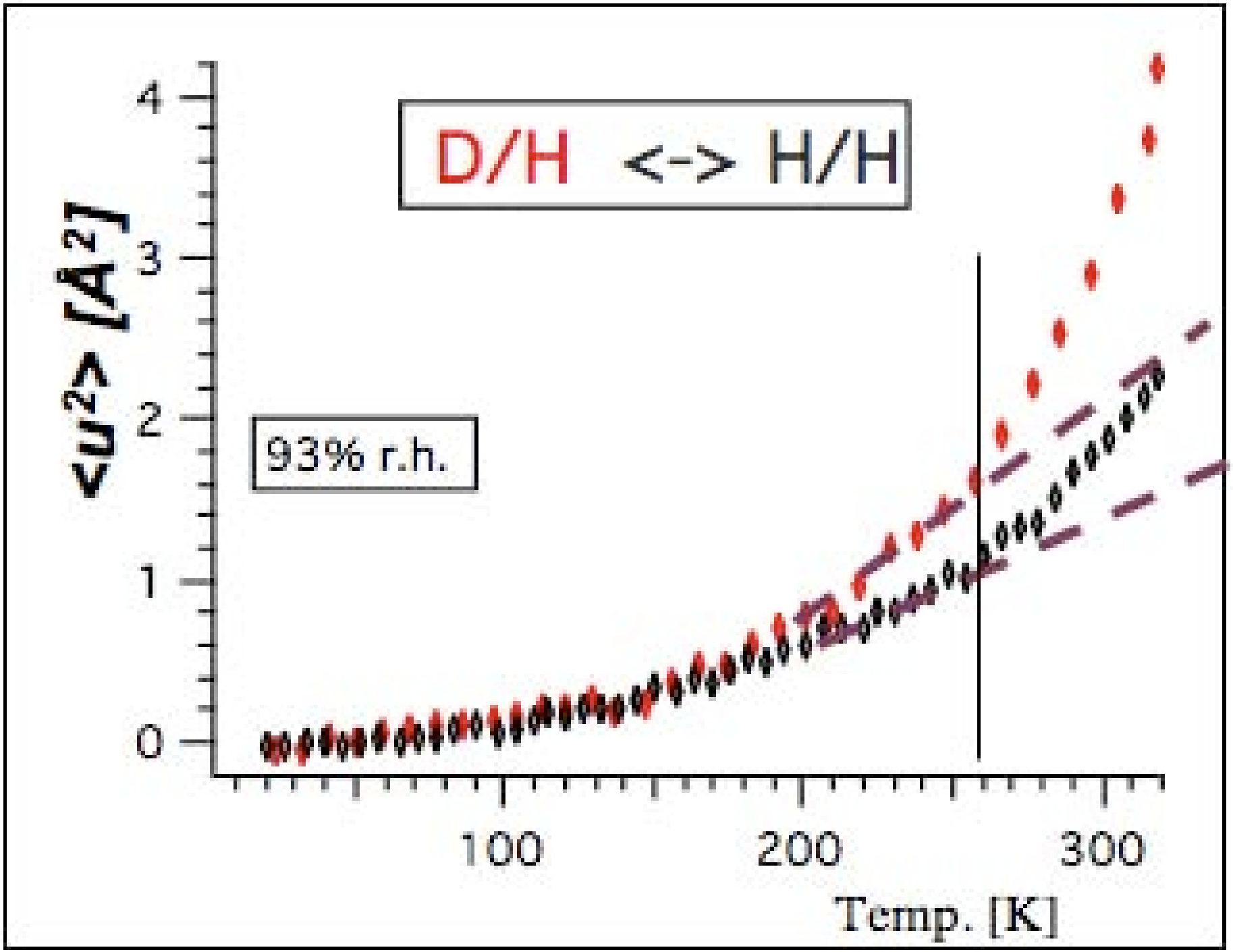

Figure 3

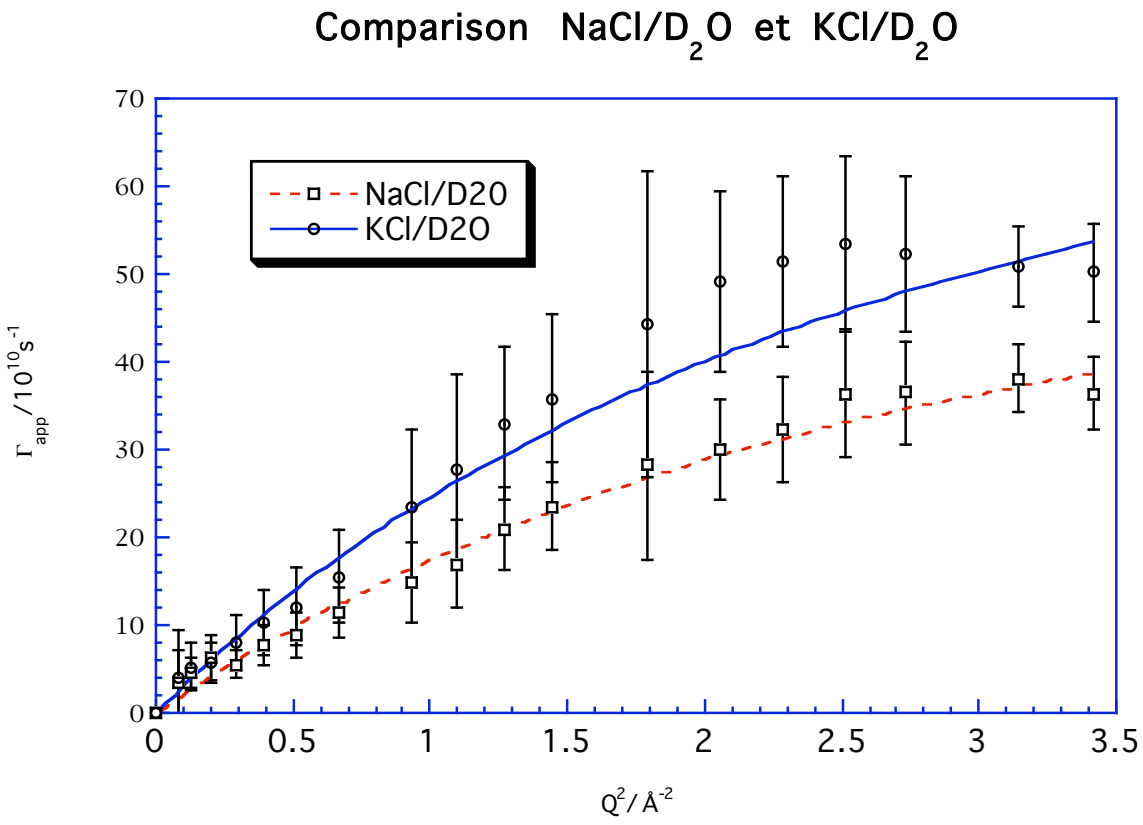
Comparison NaCl/D2O et KCl/D2O
NaCl/D20
KCl/D2O
Γapp /10^10 s^-1
Q^2 / Å^-2
0
10
20
30
40
50
60
70
0
0.5
1
1.5
2
2.5
3
3.5

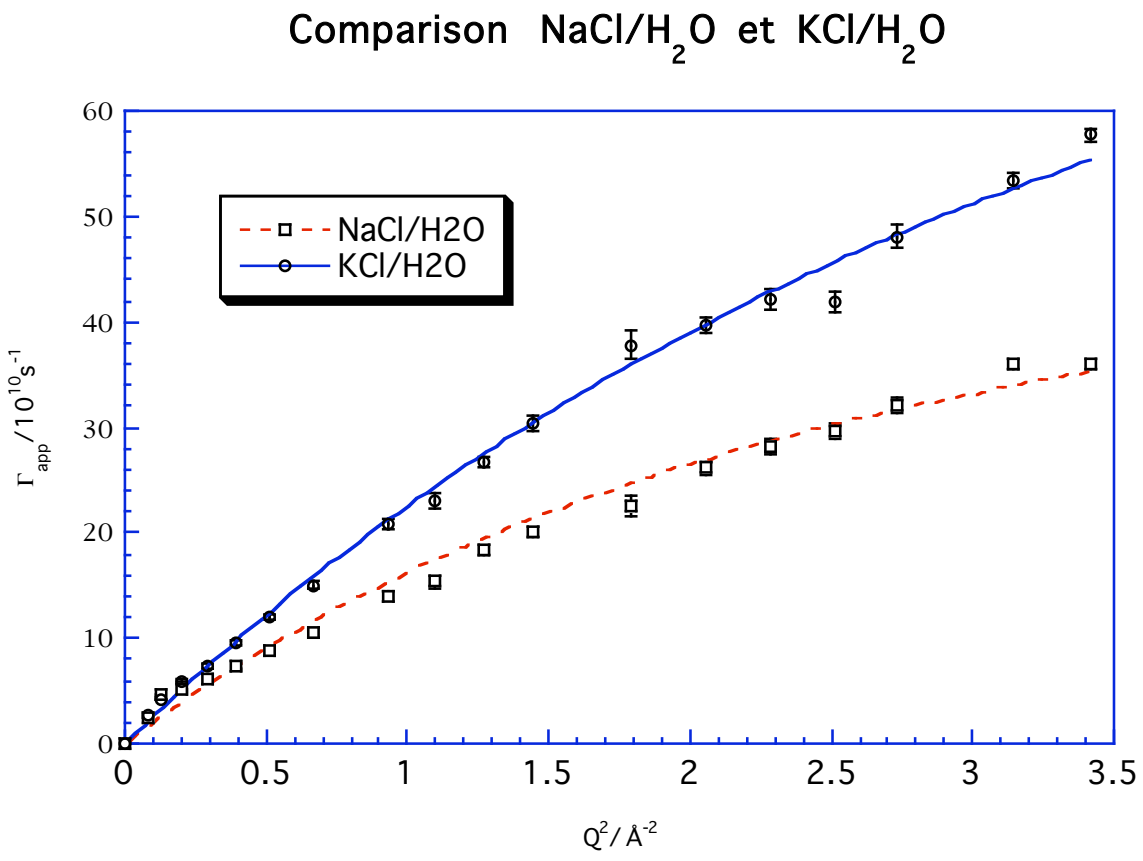
Comparison NaCl/H2O et KCl/H2O
NaCl/H2O
KCl/H2O
Γapp /10^10 s^-1
Q^2 / Å^-2
0
10
20
30
40
50
60
0
0.5
1
1.5
2
2.5
3
3.5

Figure 4

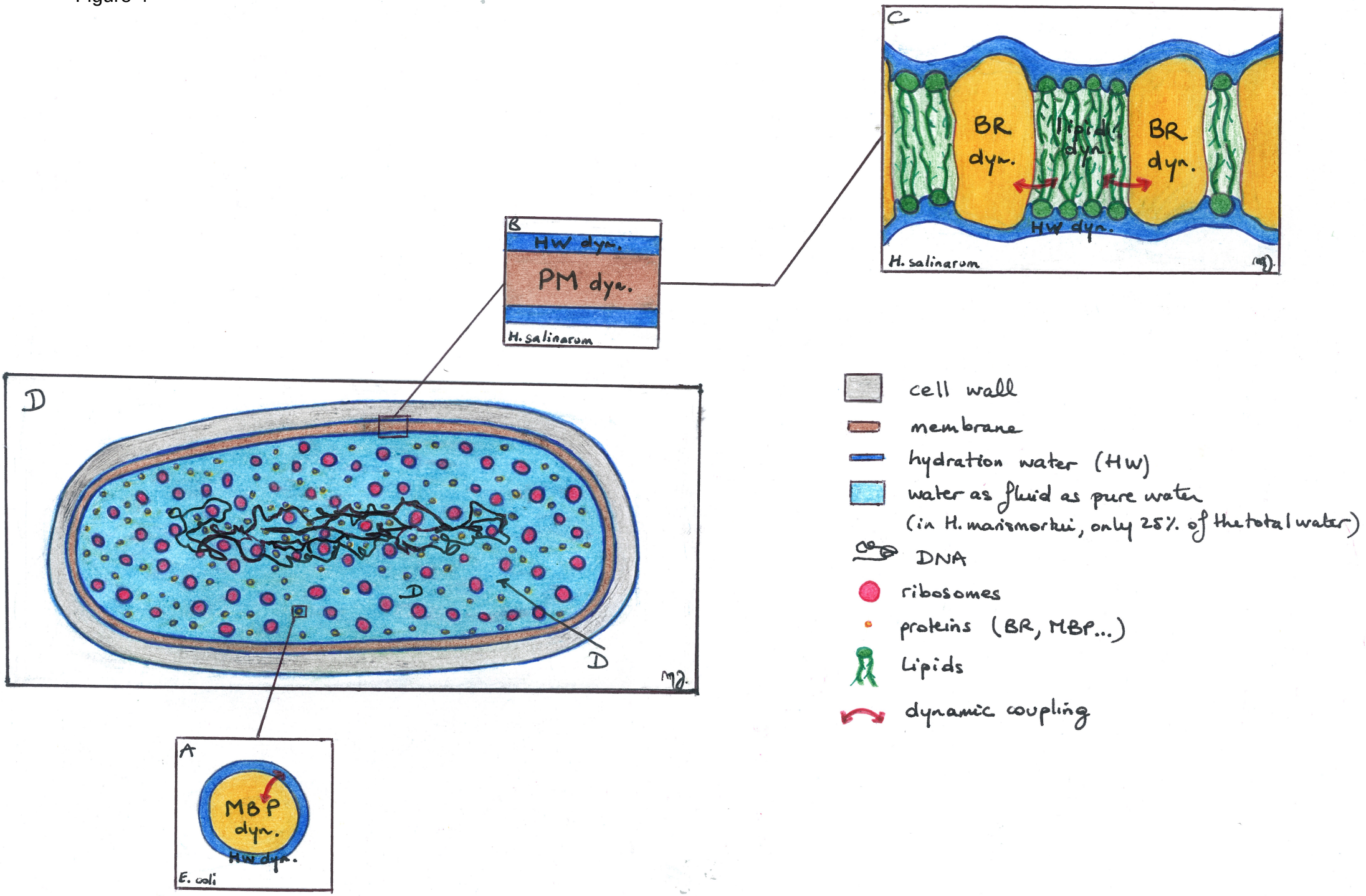
C
BR dyn.
Lipids dyn.
BR dyn.
HW dyn.
H. salinarum
B
HW dyn.
PM dyn.
H. salinarum
D
D
D
A
MBP dyn.
HW dyn.
E. coli
cell wall
membrane
hydration water (HW)
water as fluid as pure water
(in H. marismortui, only 25% of the total water)
DNA
ribosomes
proteins (BR, MBP...)
Lipids
dynamic coupling